HCCI Engine Combustion Phasing Prediction Using a Symbolic-Statistics Approach

Ahmad Ghazimirsaied*
Mahdi Shahbakhti
Charles Robert Koch†
Department of Mechanical Engineering
University of Alberta
Edmonton, Alberta T6G 2G8

Abstract

Temporal dynamics of cyclic variation in a Homogeneous Charge Compression Ignition (HCCI) engine near misfire is analyzed using chaotic theory methods. The analysis of variation of consecutive cycles of CA50 (crank angle of 50% mass fraction fuel burnt) for an n-heptane fueled engine is performed for a test point near the misfire condition. The return map of the time series of CA50 cycle values reveals the deterministic and random portions of dynamics near misfire occurring in an HCCI engine. A symbol-statistic approach is also used to find the occurrence of possible probabilities of the data points under the same operating conditions. These techniques are then used to predict CA50 one cycle-ahead. Simulated data points in phase space have similar dynamical structure to the experimental measurements.

*e-mail:ghazimir@ualberta.ca
†Corresponding author: Address: Department of Mechanical Engineering, University of Alberta, Edmonton, Alberta T6G 2G8, Canada; e-mail:bob.koch@ualberta.ca

Nomenclature

aBDC	after Bottom Dead Center
CAS	Combustion Analysis System
CA50	Crank Angle for 50% mass fraction burnt fuel
CI	Compression Ignition
COV	Coefficient of Variation
ECU	Engine Control Unit
EGR	Exhaust Gas Recirculation
EVO	Exhaust Valve Opening
HCCI	Homogeneous Charge Compression Ignition
IMEP	Indicated Mean Effective Pressure
IVC	Intake Valve Closing
Pman	Intake Manifold Pressure
PRF	Primary Reference Fuels
RPM	Revolution Per Minute
SI	Spark Ignition
SOC	Start of Combustion
TDC	Top Dead Center
Tman	Intake Manifold Temperature

1 Introduction

HCCI engines are of interest due to their advantages over conventional Spark Ignition (SI) and Compression Ignition (CI) engines. In particular, low emission levels in terms of NOx and particulate matter and high thermal efficiency of these engines are beneficial [1]. Two main concerns about this engine technology are: limited operation range, and lack of any direct control on ignition timing [2, 3, 4]. HCCI operating range is limited by the knock limit at high load and high cyclic variation at low load [5, 6]. High cyclic variations are responsible for unstable combustion and limited operating range of engine [7]. Reasons for cyclic variations are grouped in linear random, and deterministic coupling between consecutive cycles both of which have been analyzed using nonlinear and chaotic theory [8, 9, 10]. In this paper the term deterministic is used when future states for some horizon of the system can be calculated from the past values [11].

Understanding the dynamics of HCCI combustion during the high cyclic variation operating conditions can potentially be used to extend the operating range, if there is deterministic structure inherent between engine cycles. This structure can then be used to predict future cycles which can be incorporated in a control algorithm to influence ignition timing of HCCI engines [12].

Cyclic variation of HCCI is highly dependent on the timing of start of combustion [13]. Early combustion timing right after Top Dead Center (TDC) tends to have low cyclic variations of Start of Combustion (SOC) while late HCCI combustion tends to have high cyclic variations [14]. The development of period-doubling and bifurcation in the experimental measurements of spark ignition engines are investigated as the mixture is made leaner [15].

Their results indicate that there is a transition from stochastic behavior to a relatively deterministic structure as λ increases to very lean conditions. This seems to indicate that for a lean mixture conditions, cycles are related. In [16, 17], a method is proposed based on a symbolic approach to measure temporal irreversibility in time series and a new method is introduced to detect and quantify the time irreversibility. In [18], the symbolic method is analyzed in such a way so that the symbolization is used to enhance the signal-to-noise ratio. Onset of combustion instabilities under lean mixture conditions have been studied using symbolic methods for observed in-cylinder pressure measurements in SI engines [16, 19, 20]. In [21], the recent developments for applying a time-series analysis technique called symbolic time series analysis is summarized. The observation of time irreversibility in cycle-resolved combustion measurements of SI engines is discussed in [12] and the advantage of their model compared to linear gaussian random processes is presented. The transition dynamics from conventional SI combustion to HCCI combustion is described using nonlinear tools in [22], where the cyclic combustion oscillations occurring in transition between the SI and HCCI mode are presented as a sequence of bifurcations in a low-dimensional map. The sequential unstable cyclic combustion measurements in the SI-HCCI transition are used to obtain the global kinetic parameters [23]. This aids in discriminating between the multiple combustion states and to provide qualitative insight into the SI-HCCI mode transition.

The main objective of this paper is to investigate the cyclic variation of CA50 near the misfire limit in order to predict the following cycles using the identified dynamics. The results have specific implications for the control design used to stabilizing unstable HCCI operation near the misfire condition. Since the parameter CA50 is a good indicator of ignition timing [24] it is used in this work. Nonlinear and chaotic theory tools are used to identify the

inherent deterministic patterns of cyclic variation during HCCI combustion. This paper is organized into sections with the engine experimental setup described first. Then the return maps are used to qualitatively observe the dynamical patterns near the engine misfire limit. The return maps are a useful tool to recognize the dependency of the current combustion cycle on previous ones. Then the deterministic structure inherent in the data points is captured using a symbol-sequence approach. Joint probability distributions are calculated using the frequency histograms obtained in previous sections. Finally, those joint probability estimators are used to predict the next cycle ahead combustion timings in the experimental data points. Adding appropriate noise to the predicted values results in simulation results with similar statistics to the experimental data.

2 Engine Setup

A schematic of the Ricardo Hydra Mark 3 single cylinder engine fitted with a modified Mercedes E550 cylinder head is shown in Figure 1. This engine is a typical spark ignition engine with four valves per cylinder and a pent-roof combustion chamber shape. The only modification to the cylinder head is the piezo-electric pressure transducer mounted between an intake and exhaust valve. The intake air temperature can be controlled with a 600W electric heater, while the intake pressure is controlled with an externally driven supercharger. Air flow rate is measured using a laminar air flow meter mounted at the air inlet. Fuel is injected at the intake port of the engine. The fuel injection is done with a dSpace-MicroAutobox ECU (Engine Control Unit), which provides accurate control of the injection timing as well as the duration. This ECU also controls the spark timing, which is used during the engine

warm up but is turned off for HCCI combustion.

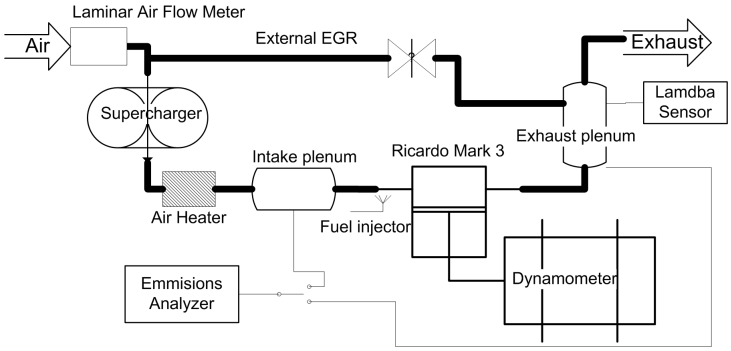

Figure 1: Schematic of the experimental setup.

Some engine specifications are listed in Table 1. Cylinder pressure is recorded 3600 times per crank revolution and processed with an A&D Baseline CAS using a degree based real time processor. At each engine cycle the relative pressure signal from the piezo-electric pressure transducer is pegged to an absolute value of pressure measured in the intake manifold. The pressure trace is then analyzed for combustion metrics, such as IMEP and CA50. These metrics are then logged for a duration of 6000 engine cycles. All other parameters, such as intake pressure and temperature, are recorded at 10 Hz using A&D Baseline DAC acquisition system.

When collecting the data for a stationary engine condition (all inputs held constant) the engine is first warmed up so that both the oil and coolant temperature remain constant.

Table 1: Configuration of the Ricardo single-cylinder engine

Parameters	Values
Bore × stroke [mm]	80 × 88.9
Compression Ratio	10
Displacement [L]	0.447
Valves	4
IVC [aBDC]	55
EVO [aBDC]	-70

3 Cycle-Ahead Prediction

The goal of this work is to predict CA50 using past and present values of CA50 for the engine operating near misfire. To do this a variety of techniques are used. First a chaotic analysis is performed on a test point at steady-state with the Coefficient of Variation of IMEP (COV_{IMEP}) of 35% for 6000 consecutive engine cycles. Then, the first half of the data (Cycles 1 to 3000) is analyzed to find the probabilistic histogram while the second portion of data (Cycles 3001 to 6000) is kept for validation. The test point is very close to complete misfire with many misfire combustion events and has only slightly larger engine torque than the motoring condition. The severity of misfire is recognized by looking at power or output torque which is too low (5 Nm in this case). A flowchart of cycle-ahead prediction based on chaotic analysis results is illustrated in Figure 2. This figure outlines the analysis procedure in the next part of the paper.

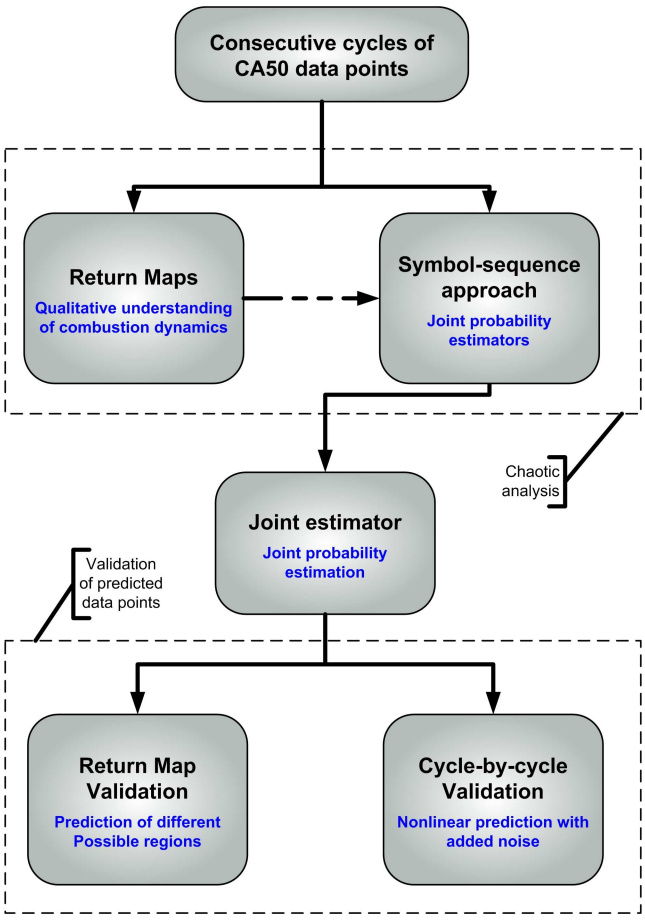

Figure 2: Flowchart: Using chaotic tools for nonlinear prediction

3.1 Return Maps

A return map can be used to observe the structures inherent in a time series [22]. Here they provide a tool to check the probable interaction between a cycle parameter and its next consecutive cycle. For a random time series, consecutive cycles are uncorrelated and the return map shows an unstructured cloud of data points gathered around a fixed point. With deterministic coupling between consecutive points the return map shows more structure such as dispersed data points about a diagonal line [25]. In this paper the analysis of HCCI engine data at an engine speed of 1000 rpm, a manifold temperature of 44 °C and a

boosted manifold pressure of 94.5 kPa is performed. The return map of all 6000 points of CA50 for this engine operating point is shown in Figure 3. A relationship of combustion

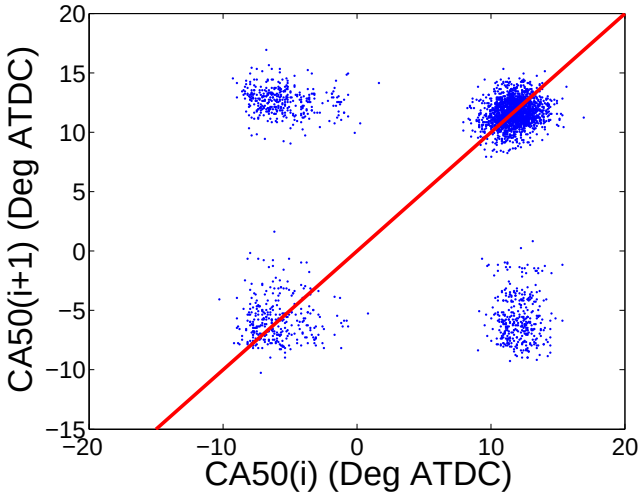

Figure 3: CA50 Return map for HCCI combustion under these conditions: engine speed 1000 rpm, Tman 44 °C, Pman 94.5 kPa, λ 2.34

phasing between the current cycle and the next cycle is shown in Figure 3 and this return map clearly shows a deterministic dependency on previous cycles. Thus to predict future cycles (for some prediction horizon) previous combustion cycles are needed. However, the detailed relationship between cycles is not apparent in the Figure 3 and it will be further discussed in the following sections. To characterize the combustion dynamics behavior, the following functional form for CA50 (at cycle i) using previous cycles is used:

$$CA50(i) = f(CA50(i-1), CA50(i-2), ..., CA50(i-L))$$

Chaotic tools such as return maps and symbol-sequence techniques are employed to find the approximate function f and value of L. Since a random time series with an unstructured

cluster of data points tends to produce a high dimensional function f [22], the return map of Figure 3 shows a relative low value of L. It can also be inferred from Figure 3 that the function f is a nonlinear function.

3.2 Symbol-sequence Analysis

In this section the symbol-sequence method is used to extract information from the experimental measurements of CA50. This method is used to detect the patterns occurring in the data points and is useful when dealing with data with high measurement error or dynamic noise [15]. Using symbol-sequence statistics requires converting the continuous phase space plots into discrete partitions [26]. Symbolization includes generating discretized symbols from raw experimental analog signals. The symbolization method is based on partitioning the original data points into finite discrete regions and each region is then attributed to a particular symbolic value. The number of possible symbols is called symbol-set size n [21, 26, 27]. After symbolization, each group of symbols form a finite-length template called the symbol sequence L. These symbol sequences consist of consecutive symbols stepping through the whole data set point by point forming a new sequence. The sequence of symbols carries some important information about the experimental measurement dynamics [16]. The total possible number of sequences N is a combination of symbol-set size n and symbol sequence length L as follows: $N = n^L$ [16].

The symbol-sequence approach also has tools to find inherent structure in experimental data points despite random-like appearance. This is performed by observing if some patterns dominant the time series, since any gaussian process, on average, would result in a flat

histogram of the N symbol-set [15].

For the HCCI data near misfire *n=8*, eight equidistant partitioning, are used which transforms the CA50 data to symbol series from 0 to 7. The data points, below the first bottom partition are assigned to symbol 0 and those higher than first bottom partition are assigned to symbol 1 and so on. The relatively high number of eight partitions selected is used to obtain detailed information out of the original data set despite that the observed dynamics is obscured with noise [26, 28].

Using the symbol-sequence approach, much of the deterministic structure inherent in the data can be captured [27]. To determine L, a joint probability distribution to predict the next cycle occurrence using previous cycles information is useful. These frequency histograms give the maximum likelihood probability of next cycle given the occurrence of previous cycles in the whole time series. Then by comparing the one-cycle ahead predictions for different values of L, the optimal value of L can be determined. These histograms also give the probabilistic function for different data series. For the engine test point with return map of Figure 3, the optimal one-step ahead prediction is found using three previous cycles ($L = 3$).

Symbol-sequence histogram for the first 3000 consecutive cycles of CA50 data of Figure 3 is shown in Figure 4. The vertical axis corresponds to normalized frequency of occurrence of this symbol sequence and horizontal axis indicates the symbol-sequence equivalent binary code. The symbol set size $n = 8$ and sequence length $L = 3$, so there are $8^3 = 512$ possible sequences.

A large normalized frequency peak accompanied by some smaller peaks in the sequence code histogram is apparent in Figure 4 which indicates non-random sequences. The large peak occurs at sequence 438 (symbol series 666) which is three consecutive late timing of ig-

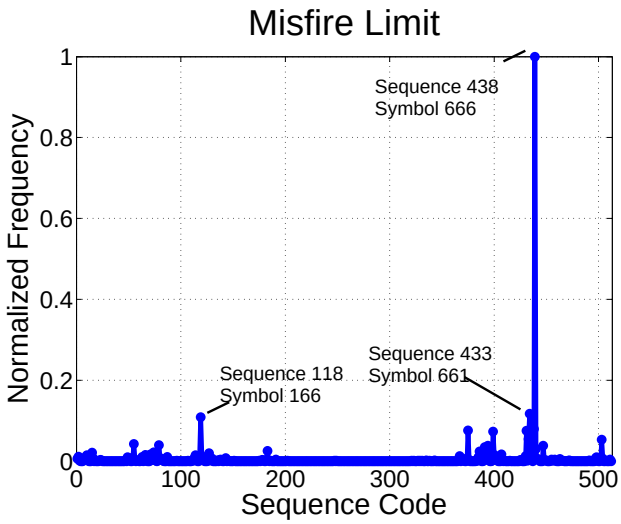

Figure 4: CA50 Symbol sequence histogram with (n=8, L=3) for HCCI combustion cycles 1 to 3000 (conditions as in Figure 3)

nition. Pattern number 433 and 118, which correspond to sequence 661 and 166 respectively, are two of main local peaks in the diagram. These cases indicate that CA50 does not stay in the late regions but oscillates between relatively early and late CA50 angle regions. In addition sequence codes 661 and 166 are among the possible sequences that the dynamics would pass through before entering or leaving three consecutive symbols of 6. These local peaks indicate relative deterministic behavior of CA50 combustion timing for the experimental case studied.

3.3 Nonlinear Prediction

Using the joint probability estimator for first half of the CA50 data (Cycles 1 to 3000) the simulated behavior of consecutive cycles of CA50 can be constructed using the deterministic part of the data captured by the model. To obtain the predicted return map, the two previous

CA50 values are used to predict the CA50 of the following cycle. The predicted return map uses the validation data (CA50 Cycles 3001 to 6000) and the resulting prediction is shown as large round symbols in Figure 5. The experimental CA50 data points are also plotted in Figure 5 using small dot symbols in order to compare the prediction to experiment. The

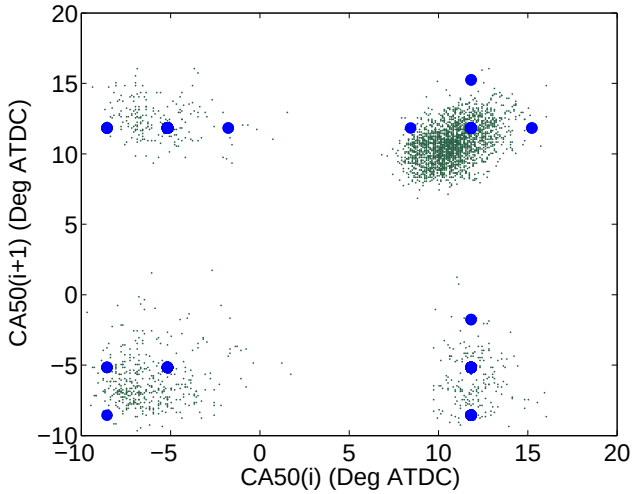

Figure 5: Comparing predicted CA50 return map to experiment (for validation data - cycles 3001 to 6000 for conditions as in Figure 3)

prediction seems to capture the nonlinear dynamics of the real data without the random variation as shown in Figure 5.

To simulate CA50 with statistics similar to the measured CA50, a random component is added to the simulated data points as:

$$CA50(i) = f(CA50(i-1), CA50(i-2), ..., CA50(i-k)) + rand(i) \qquad (1)$$

where *rand(i)* is a gaussian random variable with zero mean and a variance of $\sigma \cong 4\%$ of maximum function *f*. The experimental data for cycles 3001 to 6001 in Figure 6(a) is compared to the simulation with noise for the same cycles in Figure 6(b).

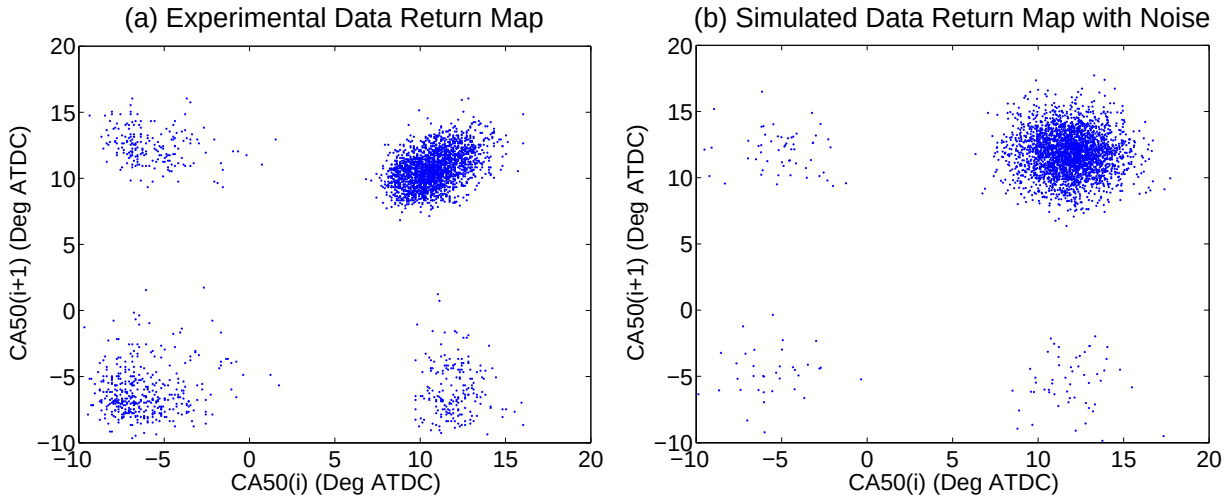

Figure 6: Simulated CA50 return map including noise compared to experimental measurements for HCCI combustion cycles 3001 to 6000 - conditions as in Figure 3

The simulated return map in Figure 6(b) has the general appearance of the experimental data in Figure 6(a).

3.4 Validation

An 800 point portion of the validation data is used to check the prediction quality. The corresponding residuals and autocorrelation function are shown in Figure 7 and Figure 8 respectively.

There is no obvious visible pattern in residuals error values in Figure 7. This indicates no dependency between consecutive error values, thus the model used to predict seems to capture the dynamics. To confirm that there is no dependency between consecutive error values, the autocorrelation function for the residuals (prediction errors) are computed and shown in Figure 8 for all the 3000 CA50 validation data points. The confidence interval for

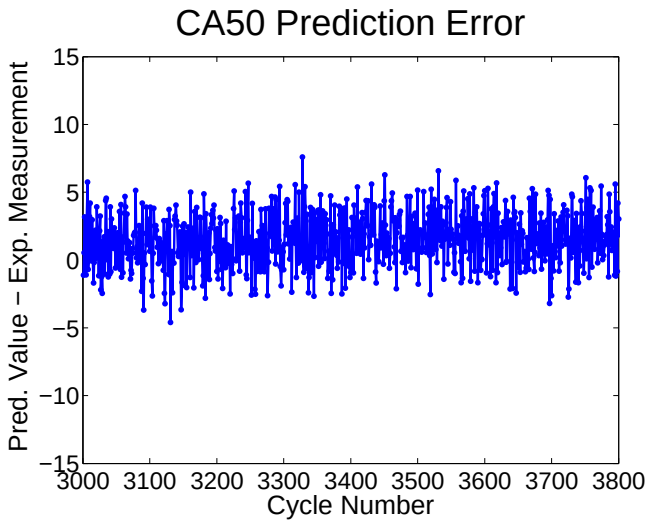

Figure 7: Prediction error between predicted CA50 values and experimental measurements for HCCI combustion - conditions as in Figure 3

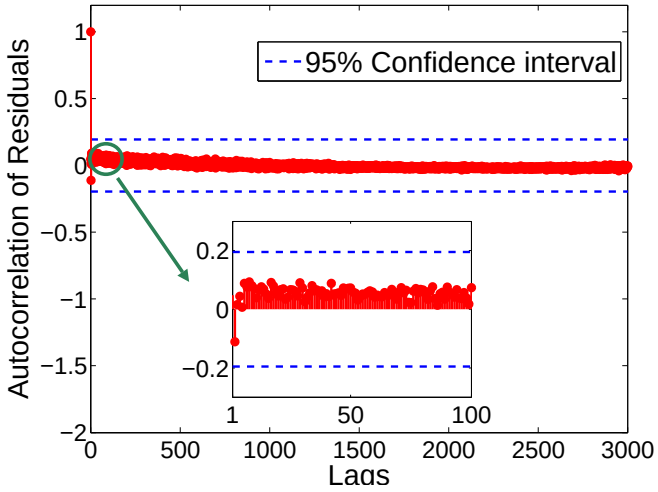

Figure 8: Autocorrelation of residuals for predicted CA50 consecutive cycles for HCCI combustion - conditions as in Figure 3

these functions is shown by dashed lines. Ideally for an acceptable model the correlation curves should fall between these lines [29] which is the case in Figure 8.

4 Conclusions

Deterministic patterns in cyclic variation of ignition timing (CA50) at one operating point near the misfire limit operation of an HCCI engine is observed. The nonlinear cluster of consecutive CA50 values near the misfire limit is illustrated in the return map consisting of multiple different regions which indicates non-constant combustion timing near the misfire limit. Considerable fluctuations in late ignition timings (CA50) occur since prior cycles affect the current cycle. Non-random patterns of cyclic variation of ignition timing under this specific operating conditions emerge in symbol sequence analysis as large peaks in the symbol-sequence histogram. A joint probability estimator to predict one cycle ahead using two previous values is developed and on validation data predicts combustion timing well. Adding random noise with the appropriate magnitude results in a simulation that looks similar to experimental measurements on a return map. An autocorrelation of predicted-actual CA50 residual shows uncorrelated residuals (with 95% confidence) which indicates the joint probability model is acceptable.

5 Future Work

For the engine operating condition tested, one cycle CA50 prediction would be extremely useful in order to modify engine inputs (and thus modify combustion CA50) in order to avoid misfire. Thus the CA50 prediction coupled with a feedback control could be used to extend HCCI combustion near misfire.

Using these predicted deterministic points could be useful in constructing the attractors that absorb the evolution of data points into finite regions. Expanding the analysis for more

operating points and extending the prediction horizon is planned.

6 Acknowledgment

The authors acknowledge the Natural Sciences and Engineering Research Council of Canada (NSERC), AUTO21 Network of Centers of Excellence, and Daimler for supporting this work. For his contributions in collecting the experimental data A. Audet [30] is gratefully acknowledged.

References

[1] Stanglmaier, R. and Roberts, C., "Homogeneous Charge Compression Ignition (HCCI): Benefits, compromises, and future engine applications," SAE Paper No. 1999-01-3682.

[2] Santoso, H., Matthews, J., and Cheng, W. K., "Managing SI/HCCI Dual-Mode Engine Operation," SAE Paper No. 2005-01-0162.

[3] Weinrotter, M., Wintner, E., Iskra, K., and Neger, T., "Optical Diagnostics of Laser-Induced and Spark Plug-Assisted HCCI Combustion," SAE Paper No. 2005-01-0129.

[4] Urushihara, T., Yamaguchi, K., Yoshizawa, K., and Itoh, T., "A Study of a Gasoline-fueled Compression Ignition Engine Expansion of HCCI Operation Range Using SI Combustion as a Trigger of Compression Ignition," SAE Paper No. 2005-01-0180.

[5] Kalaghatgi, G. and Head, R., 2006, "Combustion Limits and Efficiency in a Homogeneous Charge Compression Ignition Engines," International Journal of Engine Research, **7**, pp. 215–236.

[6] Shahbakhti, M., Lupul, R., Audet, A., and Koch, C. R., 2007, "Experimental Study of HCCI Cyclic Variations for Low-Octane PRF Fuel Blends," Proceeding of Combustion Institute/Canadian Section (CI/CS) Spring Technical Conference.

[7] Shahbakhti, M., Lupul, R., and Koch, C. R., "Cyclic Variations of Ignition Timing in an HCCI Engine," Proceedings of the 2007 ASME Internal Combustion Engine Division Spring Technical Conference (Peublo, Colorado USA).

[8] Daw, C., Finney, C., Kennel, M., and Connolly, F., 1997, "Cycle-by-cycle Combustion Variations in Spark-Ignited Engines," Proceeding of the Fourth Experimental Chaos Conference.

[9] Daw, C., Finney, C., and Green, J., "A Simple Model for Cyclic Variations in a Spark-Ignition Engine," SAE Paper No. 962086.

[10] Wagner, R., Drallmeier, J., and Daw, C., 1998, "Prior-Cycle Effects in Lean Spark Ignition Combustion - Fuel/Air Charge Considerations," SAE Special Publications, pp. 69–79.

[11] Selik, M., Baraniuk, R., and Haag, M., 2007, "Signal Classifications and Properties," Tech. rep., Work produced by The Connexions Project and licensed under the Creative Commons Attribution License.

[12] Green, J., Daw, C., Armfield, J., Finney, C., and Durbetaki, P., "Time Irreversibility of Cycle-by-Cycle Engine Combustion Variations," Proceedings of the 1998 Technical Meeting of the Central States Section of the Combustion Institute.

[13] Shahbakhti, M. and Koch, C. R., 2009, "Physics Based Control Oriented Model for HCCI Combustion Timing," Journal of Dynamic Systems, Measurement and Control, to appear.

[14] Shahbakhti, M. and Koch, C. R., 2008, "Characterizing the Cyclic Variability of Ignition Timing in a Homogenous Charge Compression Ignition Engine Fueled with N-heptane/Iso-octane Blend Fuels," International Journal of Engine Research, **9**, pp. 361–397.

[15] Wagner, R., Drallmeier, J., and Daw, C., 1998, "Origins of Cyclic Dispersion Patterns in Spark Ignition Engines," Proceedings of the 1998 Technical Meeting of the Central States Section of the Combustion Institute, pp. 213–218.

[16] Daw, C., Finney, C., and Kennel, M., 2000, "A Symbolic Approach for Measuring Temporal Irreversibility," Physical Review E, **62(2):**, pp. 1912–1921.

[17] Green, J. J., Daw, C., Armfield, J., and Finney, C., "Time Irreversibility and Comparison of Cyclic-Variability Models," SAE Paper No. 1999-01-0221.

[18] Peter, B., 2001, "Estimating and Improving the Signal-to-noise Ratio of Time Series by Symbolic Dynamics," Phys Rev E, **64**.

[19] Daw, C., Kennel, M., Finney, C., and Connolly, F., 1998, "Observing and Modeling Nonlinear Dynamics in an Internal Combustion Engine," Phys. Rev. E, **57**, pp. 2811–2819.

[20] Daw, C., Green, J., Wagner, R., Finney, C., and Connolly, F., 2000, "Synchronization of Combustion Variations in a Multi-Cylinder Spark Ignition Engine," Proceedings of the 2000 Spring Technical Meeting of the Central States Section of the Combustion Institute, pp. 181–186.

[21] Daw, C., Finney, C., and Tracy, E., 2003, "A Review of Symbolic Analysis of Experimental Data," Review of Scientific Instruments, **74**, pp. 916–930.

[22] Daw, C., Wagner, R., Edwards, K., and Green, J., "Understanding the Transition Between Conventional Spark-Ignited Combustion and HCCI in a Gasoline Engine," 31st International Symposium on Combustion (Heidelberg, Germany; August 2006).

[23] Daw, C. S., Edwards, K. D., Wagner, R. M., and Green, J. B., 2008, "Modeling Cyclic Variability in Spark-Assisted HCCI," Journal of Engineering for Gas Turbines and Power, **130**.

[24] Bengtsson, J., 2004, *Closed-Loop Control of HCCI Engine Dynamics,*, Ph.D. thesis, Lund Institute of Technology.

[25] Wagner, R. M., Daw, C. S., and Green, J. B., "Characterizing Lean Spark Ignition Combustion Instability in Terms of a Low-Order Map," Proceedings of the 2nd Joint Meeting of the U.S. Sections of the Combustion Institute.

[26] Tang, X., Tracy, E., Boozer, A., Debrauw, A., and Brown, R., 1995, "Symbol Sequence Statistics in Noisy Chaotic Signal Reconstruction," Phys. Rev. E, **51**, pp. 3871–3889.

[27] Finney, C., Green, J. J., and Daw, C., 1998, "Symbolic Time-Series Analysis of Engine Combustion Measurements," SAE Special Publications, **1330**, pp. 1 – 10.

[28] Tang, X., Tracy, E., and Brown, R., 1997, "Symbol Statistics and Spatio-Temporal Systems," Physica D, **102:**, pp. 253–261.

[29] "NIST/SEMATECH e-Handbook of Statistical Methods http://www.itl.nist.gov/div898/handbook/," .

[30] Audet, A., 2008, *Closed Loop Control of HCCI Using Camshaft Phasing and Dual Fuels*, Master's thesis, University of Alberta.

List of Table Captions

List of Figure Captions

1. Figure 1: Schematic of the experimental setup
2. Figure 2: Flowchart: Using chaotic tools for nonlinear prediction
3. Figure 3: CA50 Return map for HCCI combustion under these conditions: engine speed 1000 rpm, Tman 44 °C, Pman 94.5 kPa, λ 2.34
4. Figure 4: CA50 Symbol sequence histogram with (n=8, L=3) for HCCI combustion cycles 1 to 3000 (conditions as in Figure 3)
5. Figure 5: Comparing predicted CA50 return map to experiment (for validation data - cycles 3001 to 6000 for conditions as in Figure 3)
6. Figure 6: Simulated CA50 return map including noise compared to experimental measurements for HCCI combustion cycles 3001 to 6000 - conditions as in Figure 3
7. Figure 7: Prediction error between predicted CA50 values and experimental measurements for HCCI combustion - conditions as in Figure 3
8. Figure 8: Autocorrelation of residuals for predicted CA50 consecutive cycles for HCCI combustion - conditions as in Figure 3